MULTIPLE NUMERICAL SOLUTIONS OF BUOYANCY INDUCED FLOWS OF A VERTICAL ICE WALL MELTING IN SATURATED POROUS MEDIA

C.-A. WANG

Department of Applied Mathematics, National Chiao Tung University, Hsinchu, Taiwan 30050, R.O.C.

Communicated by E. Y. Rodin

Abstract—A mathematical model of buoyancy induced flows next to a vertical wall of ice melting in porous media saturated with water is studied. With the boundary layer approximation and a similarity transformation, a two-point boundary value problem (BVP) is formed and, then, studied by the multiple shooting code BVPSOL. Numerical solutions are found in two disjoint regions of ambient water temperature for various salinity levels. In each region, solutions are obtained by applying the continuity process which gives, respectively, a smooth bifurcation curve of the appropriate parameter. Multiple solutions are found at some ambient temperatures in these two regions. Some of them are similar. The others indicate physically the potential existence of a large amount of energy for any trend arising that drives one flow state to another.

NOMENCLATURE

A, B, P, Q = Variables in buoyancy term
c_p = Specific heat
D = Diffusivity
E, H = Ancillary functions
f = Similarity stream function
g = Gravitational acceleration
g_1, g_2, g_3 = Coefficients of some expressions
h_{il} = Latent heat
k = Integration constant
$k1, k2$ = Functions in boundary condition
K = Permeability of porous media
n = Porosity of porous materials
q = Exponent in density relation
R = Temperature ratio
Ra_x = Local Rayleigh number
s = Salinity
S = Similarity function of salinity
t = Temperature
u = Darcy velocity in x-direction
v = Darcy velocity in y-direction
V = Vector velocity
W = Buoyancy function
x = Coordinate tangent to the ice wall
y = Coordinate normal to the ice wall
α = Coefficient in density relation
α_1 = Thermal-diffusivity ratio
$\beta = \alpha_1 - 1$
ϕ = Normalized similarity function of temperature
η = Independent similarity variable
κ = Thermal conductivity
μ = Viscosity of fluid
ρ = Density
τ = Time
ψ = Stream function

Subscripts

a = Motion of fluid
e = Effective quantities of porous media
f = Quantities of fluid
i = Quantities of ice

m = Quantities at extreme
r = Quantities at reference condition
s = Quantities of porous material
U,L = Upper and lower solutions at the same ambient temperature or R
1, 2 = Lower and upper bound of the gap in R
0 = Quantities at the interface
∞ = Quantities at infinity

1. INTRODUCTION

In the natural world, transport processes in fluids where the motion is driven by the interaction of a difference in density in a gravitational field are common. Usually, density variation is caused by temperature differences. As in oceanic circulation, the differences in salinity may further affect the density. Therefore, the buoyancy force is the stimulus to the fluid flow, particularly in oceanic circulation. Such flows are called "natural convection".

The mechanisms of such flows are complicated by the occurrence of density extrema as the temperature varies [1]. It is known that a density extremum is reached at about 4°C in pure water at atmospheric pressure. A density extremum also occurs in saline water up to a salinity level of about 26 p.p.t. (parts per thousand) and at an elevated pressure up to 300 bars absolute.

Such mechanisms also occur in fluid saturated porous media such as permeable soils flooded by cold lake or sea water, or water slurries, since density extrema may occur in this situation as well. Ramilison and Gebhart [2] presented a study of the problem of transport of porous media saturated with cold pure or saline water at a low temperature, with a density relation as in Ref. [3]. Meanwhile, a temperature ratio R was introduced, $R = (t_m - t_\infty)/(t_0 - t_\infty)$, with an ambient temperature t_∞, a density extremum temperature t_m and a temperature at the vertical surface t_0. The reported that the existence of a gap in R where no similarity steady state solution is obtained. Gebhart et al. [4] then presented a more delicate numerical study to obtain new solutions and improved the accuracy of gap in R to appropriate parameters and multiple solutions with greatly different characteristics at the same R are found. These results were verified rigorously by Hastings and Kazarinoff [5].

It was concluded that, in Refs [2] and [4], both flow and buoyancy force are upward for $R < 0$ and downward for $R > 1/2$. For R ranging from 0 to 1/2, two distinct flow regimes with a local buoyancy force reversal across the thermal diffusion region have also been found. The flow is the first regime, for values of R near 0, is mostly upward, as in Fig. 1(a), and mostly downward in the second the regime with R close to 1/2, as in Fig. 1(b).

Note that the studies of Refs [2] and [4] have been restricted to the case of an isolated vertical ice surface in the sense that none of melting, freezing or salinity diffusion is allowed. Carey [6] presented experimental and numerical studies on the problem of a vertical ice melting in saline water, and indicated the importance of salinity diffusion when the melting process is taking place.
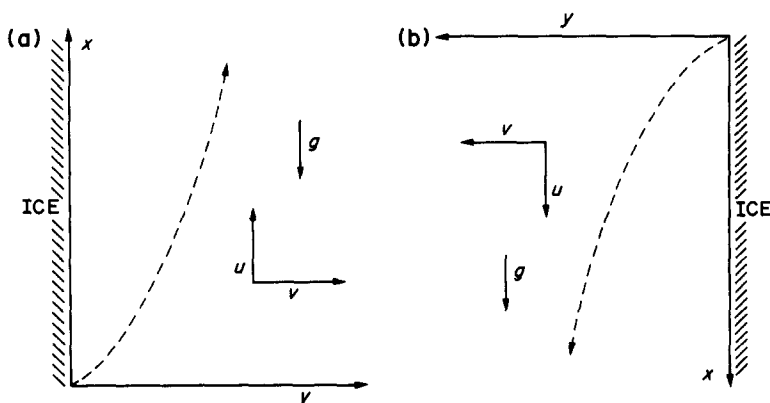

Fig. 1. Coordinate systems for two flow regimes (a) the mostly upward flow and (b) the mostly downward flow.

It is our purpose here to study the effect of salinity diffusion to a problem of a vertical ice wall melting in porous media saturated with water.

2. MODEL AND ANALYSIS

Consider a vertical wall of ice melting in an isotropic and homogenous porous medium. The concentration of salt s is assumed to be small comparing with the density of water. The Soret and Dufour effects are neglected. The cartesian coordinate system is taken with the origin at the leading edge of ice, where the x-direction is taken positive in the direction of upstream (or downstream) and the y-direction is taken normal to the ice surface, as Fig. 1(a) [or Fig. 1(b)]. When the coordinate system taken as stationary relative to the far ambient medium, the ice water interface moves in the negative y-direction with velocity $V_i(x)$ as the ice melts. Thus, the flow field is time dependent and, by the order-of-magnitude argument, this time dependence has an effect $O(1)$ even at low ambient temperature which results in low melting rate.

Let u and v be vertical and horizontal components of the Darcy velocity: K be the permeability of the porous medium: μ, c_p and ρ_r be the viscosity, specific heat and density of the convective fluid at the reference condition: k_e and D_e be the effective thermal conductivity of the saturated porous medium and the effective diffusivity of salt in the porous medium saturated with saline water. Also the fluid pressure and the gravitational acceleration are denoted by p and g.

As the Boussinesq approximation is applied, the governing time dependent equation, due to Ramilison and Gebhart [2], Carey [6], and Gebhart and Mollendorf [3] are given as follows:

$$\frac{\partial u}{\partial x} + \frac{\partial v}{\partial y} = 0; \tag{1}$$

$$\frac{\partial u}{\partial \tau} + u = \frac{K}{\mu}\left(\pm \rho g - \frac{\partial p}{\partial x}\right); \tag{2a}$$

$$\frac{\partial v}{\partial \tau} + v = -\frac{K}{\mu}\frac{\partial p}{\partial y}; \tag{2b}$$

$$\frac{\partial t}{\partial \tau} + u\frac{\partial t}{\partial x} + v\frac{\partial t}{\partial y} = \frac{k_e}{\rho_r c_p}\left[\frac{\partial^2 t}{\partial x^2} + \frac{\partial^2 t}{\partial y^2}\right]; \tag{3}$$

$$\frac{\partial s}{\partial \tau} + u\frac{\partial s}{\partial x} + v\frac{\partial s}{\partial y} = D_e\left[\frac{\partial^2 s}{\partial x^2} + \frac{\partial^2 s}{\partial y^2}\right]; \tag{4}$$

$$\rho = \rho_m(s,p)[1 - \alpha(s,p)|t - t_m(s,p)|^{q(s,p)}], \tag{5}$$

where ρ_m is the extreme of the fluid density, t_m is the temperature at which ρ_m occurs and τ denotes the time.

The phase change will cause the ambient fluid in the porous medium to move toward the ice wall with the constant velocity V_a. But both V_a and the interface velocity V_i are determined by melting rate, and related by

$$V_a = V_i\left[1 - \frac{\rho_i}{\rho_r(1 - s_0/1000)}\right], \tag{6}$$

where s_0 is the salinity at the interface along with uniform temperature t_0. Meanwhile, ρ_i denotes the ice density and V_i is assumed to be independent of time and entire ice mass is at temperature t_0. The boundary conditions, at small time $\tau > 0$, are

$$\text{at} \quad y = -V_i\tau; \quad ; \quad u = 0, \quad t = t_0, \quad s = s_0;$$

$$\text{as} \quad y \to \infty; \quad u \to 0, \quad t \to t_\infty, \quad s \to s_\infty. \tag{7}$$

Now, the boundary conditions (7) is transformed to a fixed ice salined water boundary in time by letting

$$x = \bar{x}, \quad y = \bar{y} - V_i\bar{\tau}, \quad \tau = \bar{\tau},$$

$$u = \bar{u}, \quad v = \bar{v} - V_i, \quad t = \bar{t}, \quad s = \bar{s}.$$

It is assumed that the coordinate system is moving with the interface, the flow field is independent of time and $V_i^{-1}(dV_i/dx)$ is small and may be neglected. For the boundary layer approximation applied here, it is assumed that the convection takes place within a thin layer adjacent to $y = 0$. Hence, by neglecting changes of physical quantities $\partial^2/\partial x^2$, compared to those with respect to y, and by dropping the bars, the governing equations (1)–(4) become

$$\frac{\partial u}{\partial x} + \frac{\partial v}{\partial y} = 0, \tag{8}$$

$$\frac{\partial u}{\partial y} = \frac{K}{\mu}\left(\pm g\frac{\partial \rho}{\partial y}\right), \tag{9}$$

$$u\frac{\partial t}{\partial x} + v\frac{\partial t}{\partial y} = \frac{k_e}{\rho_r c_p}\frac{\partial^2 t}{\partial y^2}, \tag{10}$$

$$u\frac{\partial s}{\partial x} + v\frac{\partial s}{\partial y} = D_e\frac{\partial^2 s}{\partial y^2}, \tag{11}$$

with the associate boundary conditions

$$\text{at}\quad y = 0; \quad u = 0, \quad v = V_0(x), \quad t = t_0, \quad s = s_0;$$

$$\text{as}\quad y \to \infty; \quad u \to 0, \quad t \to t_\infty, \quad s \to s_\infty, \tag{12}$$

were V_0 is the blowing velocity at the interface. From the conservation of mass and thermal energy at the interface,

$$V_0 = V_i\frac{\rho_i}{\rho_r(1 - s_0/1000)} = \frac{k_e\left.\dfrac{\partial t}{\partial y}\right|_{y=0}}{\rho_r h_{il}(1 - s_0/1000)}, \tag{13}$$

where h_{il}, the latent heat of fusion of ice, is 79.77 cal/g. Moreover, the conservation of salt and water at the interface should be included which yields

$$\frac{k_e s_0}{h_{il}}\left.\frac{\partial t}{\partial y}\right|_{y=0} = \frac{D_e\rho_r}{1 - (s_0/1000)}\left.\frac{\partial s}{\partial y}\right|_{y=0}. \tag{14}$$

Moreover, equation (9) is equivalent to

$$-u(x, y) = \pm\frac{K}{\mu}g(\rho_\infty - \rho), \tag{15}$$

by applying the integration along with the condition (12). As in Ref. [2], similarity independent variable $\eta = \eta(x, y)$ and three similarity dependent variable $f(\eta)$, $\phi(\eta)$ and $S(\eta)$ are introduced as follows:

$$\eta(x, y) = y\sqrt{Ra_x}/2x, \quad f(\eta) = \psi(x, y)/(\alpha_1\sqrt{Ra_x}),$$

$$\phi(\eta) = (t(x, y) - t_\infty)/(t_0 - t_\infty), \quad S(\eta) = (s_\infty - s(x, y))/s1,$$

where $s1 = 1$ p.p.t. and Ra_x is a local Raleigh number defined as

$$Ra_x = 2\alpha(s_\infty, p)K\rho_m(s_\infty, p)gx|t - t_\infty|^{q(s_\infty, p)}/(\mu\alpha_1),$$

with $\alpha_1 = k_e/(c_p\rho_r)$. Also $\psi(x, y)$ is the usual stream function with $\partial\psi/\partial y = u$ and $\partial\psi/\partial x = -v$. Hence, $u(x, y) = (\alpha_1 Ra_x/2x)f'(\eta)$, $-v(x, y) = (\alpha_1\sqrt{Ra_x}/2x (f - nf')$. Therefore, equations (5), (8), (10), (11) and (15) with boundary conditions (12)–(14) are transformed to an autonomous system

$$f'(\eta) = \pm W(\phi, R, S), \tag{16\pm}$$

$$\phi''(\eta) + f(\eta)\phi'(\eta) = 0, \tag{17}$$

$$S''(\eta) + (\alpha_1/D_e)f(\eta)S'(\eta) = 0, \tag{18}$$

with boundary conditions

$$\phi(0) = 1, \quad \phi(\infty) = 0, \quad s(\infty) = 0, \quad s(0) = (s_\infty - s_0)/s1,$$

$$f(0) = c_p(t_\infty - t_0)\phi'(0)/[h_{il}(1 - s_0/1000)],$$

$$s'(0)/\phi'(0) = k_e(t_\infty - t_0)s_0/[h_{il}\rho_r D_e(1 - s_0/1000)]. \tag{19}$$

Moreover,

$$W(\phi, R, S) = (1 + AS)(1 + BS)|\phi - R - QS|^q - |R|^q - PS, \tag{20}$$

where $q = q(0, 1) = 1.894816$ and R is defined as

$$R = \frac{t_m(s_\infty) - t_\infty}{t_0 - t_\infty},$$

with $t_m(s_m) = t_m(0, 1)(1 + s_\infty g_3)$. Variables A, B, Q and P are defined by

$$A = -g_1/(1 + s_\infty g_1),$$

$$B = -g_2/(1 + s_\infty g_2),$$

$$Q = -g_3 t_m(0, 1)/(t_\infty - t_0)$$

and

$$P = A/[\alpha(0, 1)(1 + s_\infty g_2)|t_0 - t_\infty|^q],$$

where $\rho_m(0, 1) = 0.999972\ \mathrm{gcm}^{-3}$, $\alpha(0, 1) = 9.297173 \times 10^{-6}$ (°C)$^{-q(0, 1)}$, $t_m(0, 1) = 4.029325$°C, $g_1 = 0.846157 \times 10^{-3}$, $g_2 = -0.2839092 \times 10^{-2}$ and $g_3 = -0.5265509 \times 10^{-1}$. Let $P_{s_\infty}^+$ and $P_{s_\infty}^-$ denote the problems (16$^+$)–(19) and (16$^-$)–(19), respectively.

Note that the expressions for A, B, Q and P are slightly different from those in Ref. [6]. This is due to the different similarity dependent variable $S(\eta)$. Carey [6] defined it as $S^*(\eta) = (s(x, y) - s_\infty)/(s_0 - s_\infty)$ which leads to difficulty in continuing the ice melting in saline water from that in pure water. However, the system studying here will overcome such difficulty sing $S(\eta)$ is identically zero if $s_\infty = s_0 = 0$. Hence, this enables us to study the case of saline water as a perturbation of the pure water case. Moreover, due to Fujino et al. [7] and Carey [6], t_0 is assumed to be in terms of s_0 and $t_0(0) = 0$. Therefore, R, in terms of s_∞, t_∞ and s_0, should not be considered as a free parameter for the general case of $s_\infty > 0$.

Similar to Ref. [4], $\phi(\eta)$ can be taken as a new independent variable since it is strictly decreasing on $(0, \infty)$. Let $E(\phi(\eta)) = -\phi'(\eta)$ and $H(\phi(\eta)) = S(\eta)$. Then the system P_{s_∞} can be transformed to Q_{s_∞}

$$E''(\phi) = \mp W(\phi, R, \phi)/E(\phi), \tag{21$^\pm$}$$

$$H'(\phi) = \beta H'(\phi)E'(\phi)/E(\phi), \tag{22}$$

with the associated conditions

$$E(0) = 0, \quad E'(1) = k1(s_\infty, t_\infty, s_0)E(1),$$

$$H(0) = 0, \quad H(1) = (s_\infty - s_0)/s1,$$

$$H'(1) = k2(s_\infty, t_\infty, s_0), \tag{23}$$

where $\beta = (\alpha_1/D_e) - 1$, $k1(s_\infty, t_\infty, s_0) = -c_p(t_\infty - t_0)/[h_{il}(1 - s_0/1000)]$ and $k2(s_\infty, t_\infty, s_0) = k_e(t_\infty - t_0)s_0/[h_{il}D_e\rho_r(1 - s_0/1000)]$. The "shooting" method is used to study the system Q_{s_∞} and, then, $E'(0)$, $H'(0)$ and s_0 are taken as free parameters to satisfy the conditions at $\phi = 1$, if s_∞ and t_∞ are given. Note that equation (22) is equivalent to

$$H'(\phi) = kE(\phi)^\beta, \tag{24}$$

with k as an integration constant which gives the propriate parameter to overcome the difficulty in requiring that $H'(0) = 0$. Hence, the problems of (21$^\pm$), (23) and (24), denoted by $Q_{s_\infty}^\pm$, respectively, will meet the requirement of the shooting method.

Furthermore, coefficients k_e and D_e depend on the type of the porous medium. An isotropic porous medium may have several types of thermal conduction such as "parallel", "series" or even more complicated conditions. To simplify our study here, a series conduction is assumed for the

porous medium. Therefore, k_e can be written as

$$1/k_e = n/k_f + (1 - n)/k_s,$$

where k_f and k_s are the thermal conductivity of the fluid and solid in such medium, and n denotes the porosity of the solid [8]. As to k_f, an explicit form by Caldwell [9] is chosen to evaluate it. But we are unable to obtain any explicit form to evaluate k_s. Nevertheless, Somerton [10] has presented some sample data for k_s at the temperature 32°C. Hence, we have assumed that the porous medium is like well-distributed sandstone with the porosity $n = 40\%$ and set k_s to be 0.9086×10^{-2} cal/cm   s °C. Meanwhile, D_e can be formulated by [8] $D_e = k_e/[(1 - n)\rho_s c_s + n\rho_r c_p]$, where ρ_s and c_s denote the density and specific heat of the solid in the given medium. As above we set, for such special medium, $\rho_s = 1.8423$ g/cm^3 and $c_s = 0.3742446$ cal/g°C. Moreover, two explicit forms by Bromley et al. [11] and Gebhart and Mollendorf [3], respectively, are used to evaluate c_p and ρ_r at the reference temperature $t_r = (t_\infty + t_0)/2$ and salinity $s_r = (s_\infty + s_0)/2$.

3. NUMERICAL STUDY AND RESULT

Numerical computations are performed on CYBER 730 at SUNY/Buffalo by using the code BVPSOL [12–15]. BUPSOL is a multiple shooting code for solving boundary value problem in ordinary differential equation. For dealing with the stiff system, and integrator subroutine METAN1 [16–18] is imposed which is based on the semi-implicit midpoint method associated with the step size controlled by the extrapolation method.

To solve the problem Q_{s_∞}, a local accuracy controlling parameter EPS is set to be 10^{-8}. The continuity process with an appropriate parameter is applied with the initial guesses are taken by the interpolation of data obtained from the previous three runs. Due to physical interest, t_∞ in ranging from the left end $t_\infty = t_m(s_\infty)$, $R = 0$, for various level of salinity $s_\infty \geqslant 0$.

To the pure water model, it is equivalent to study the reduced problem Q_0

$$E'' = \mp w(\phi, R)/E(\phi), \tag{25$\pm$}$$

$$E(0) = 0, \quad E'(1) = k1(0, t_\infty, 0)E(1), \tag{26}$$

where $w(\phi, R) = |\phi - R|^q - |R|^q$, since $s_\infty = s_0 = k = 0$. The corrected condition at $\phi = 0$ is imposed and computations are facilitated by using the asymptotic value of $E(\phi)$, $E(\phi) \approx E'(0)\phi$, for ϕ small. When t_∞ is close to t_m, a continuous family of solution of Q_0^+ is obtained with the parameter $E'(0)$ down to 4×10^{-5}. Moreover, a smooth curve which corresponds to solutions of Q_0^- has also found with the other parameter $E(1)$ down to 10^{-6} when t_∞ is close to $2t_m(0)$, $R \sim 1/2$. It is found that a gap in t_∞ such that neither Q_0^+ nor Q_0^- has a solution.

The case $s_\infty = 10^{-4}$ has then been studied. Similar continuous families of solutions for Q_{s_∞} are also obtained and the data agree with those in the pure water model to at least 4 digits. This suggests that the case of small s_∞ is a perturbation of the pure water case. Bifurcation diagrams of t_∞ against $f(\infty)$, $-\phi'(0)$, k and s_0 will not be shown here. But they are similar to those of the case $s_\infty = 25.4$ [as Fig. 4(a)–4(d')], which will be discussed later] expect for differences of position. By setting $\alpha = E'(0) = f(\infty)$, the observed properties can be characterized, for sufficiently small $s_\infty \geqslant 0$, as follows.

1. There is a gap in t_∞, $t_1(s_\infty) < t_\infty < t_2(s_\infty)$, on which neither $P_{s_\infty}^+$ nor $P_{s_\infty}^-$ has a solution.
2. There exists a smooth curve C_0 in the $(s_\infty, \alpha, t_\infty, k, s_0)$ space such that every point on C_0 corresponds to a solution of $P_{s_\infty}^+$ with $t_\infty = t_m(s_\infty)$.
3. $P_{s_\infty}^+$ has a unique solution when t_∞ is close to $t_m(s_\infty)$.
4. It is conjectured that there is a curve Γ_{s_∞} in the $(\alpha, t_\infty, k, s_0)$ space such that each point on the curve corresponds to a solution of $P_{s_\infty}^+$ for each $s_\infty > 0$. Γ_{s_∞} is of the form $\{(\alpha, t_\infty(\alpha), k(\alpha), s_0(\alpha)) | 0 \leqslant \alpha \leqslant \alpha_0(s_\infty)\}$, where the endpoint or Γ_{s_∞} with $\alpha = \alpha_0(s_\infty)$ corresponds to a unique solution of $P_{s_\infty}^+$ if $t_\infty = t_m(s_\infty)$.
5. We also conjecture that there is curve C_1 in the $(s_\infty, \alpha, t_\infty, k, s_0)$ space such that each point on C_1 corresponds to a solution of $P_{s_\infty}^+$ when $f(\infty) = 0$. Furthermore, for each s_∞, $P_{s_\infty}^+$ has multiple solutions with $t_\infty = \bar{t}_\infty(s_\infty)$ where $\bar{t}_\infty$ is the

t_∞-component of a point on C_1. In particular, P_0^+ has infinitely many solutions at $t_\infty = \bar{t}_\infty(0)$.

6. There is a number $\bar{t}_\infty(s_\infty) > t_2(s_\infty)$ such that $P_{s_\infty}^-$ has a unique solution if $t_\infty \geq \bar{t}_\infty(s_\infty)$, and has even number solutions for t_∞ in $[t_2(s_\infty), \bar{t}_\infty(s_\infty)]$ in a sense roughly equivalent to counting of roots of a polynomial.

7. By observing the bifurcation diagram $-\phi'(0)$ vs t_∞, [as Fig. 4(b) and 4(b')] the further conjecture should be noted here. At the left region of t_∞, the bifurcation curve spirals inward and clockwise to a certain point. However, the lower branch of right hand bifurcation curve approaches to $\bar{t}_\infty(s_\infty)$ as $-\phi'(0)$ decreases to zero.

Note that, by restating with the temperature ratio R, the result of $s_\infty = 0$ is similar to the one in Ref. [4]. The correlation betwen C_0, C_1, Γ_{s_∞} and Γ_0 can be exhibited by Fig. 2. This figure and some of above properties are justified mathematically by Wang [19].

To study the cases of moderate salinity, s_∞ has been set to be 1, 10, 20 and 25. Two families of solutions of P_{s_∞} for each s_∞ are obtained successfully with significant CPU time. For each s_∞, Properties 1, 3, 4 and 6 are obtained. It is found that, as in Fig. 3(a), the width of gap in t_∞ is increasing as s_∞ increases. Meanwhile, the width of gap in R first vanishes at about $s_\infty = 25$, see Fig. 3(b). Moreover, Property 6 is also true when replacing t_∞ by R for $s_\infty = 1$, 10 and 20. But $P_{s_\infty}^-$ has only one solution for each R in $(R_2, \bar{R})$ at $s_\infty = 25$. The bifurcation diagrams of $f(\infty)$, $-\phi'(0)$, k and s_0 against t_∞ are similar except for differences of the position.
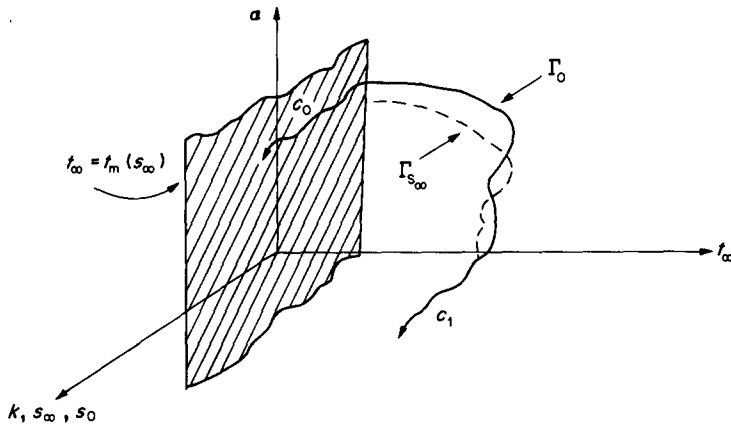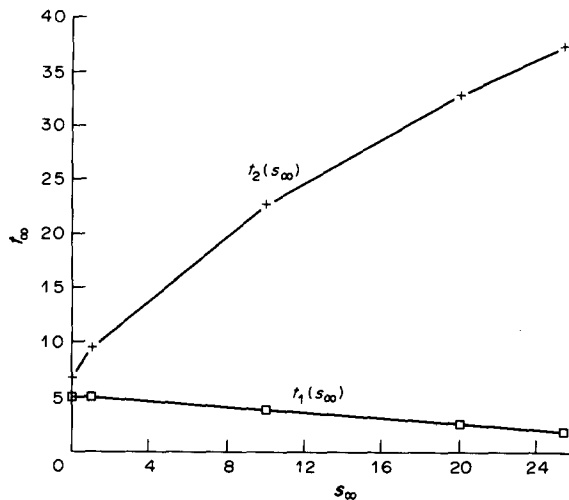

Fig. 2. The correlation between C_0, C_1, Γ_0 and Γ_{s_∞}.

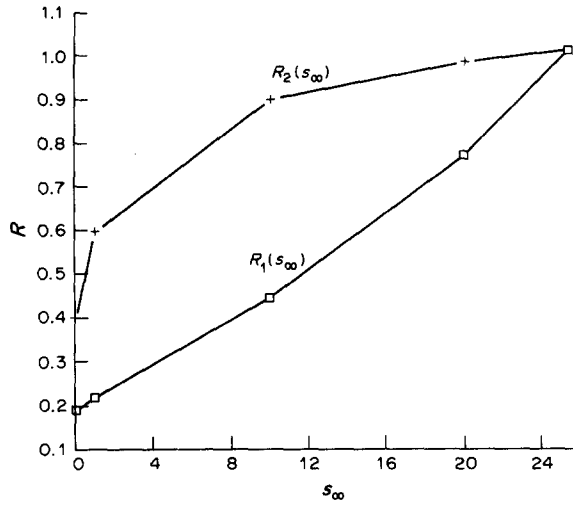Fig. 3(a). The bounds of the gap in t_∞, $t_1(s_\infty) < t_\infty < t_2(s_\infty)$.

Fig. 3(b). The bounds of the gap in R, $R_1(s_\infty) < R < R_2(s_\infty)$.

Furthermore, it is found that $t_m(s_\infty)$ is decreasing in s_∞ and negative s_∞ is greater than 19 p.p.t. This enlarges the variable $-P$ in studying the problem $P_{s_\infty}^+$. For example, $-P$ is ranging from 8 to 12.4 when $s_\infty = 20$. Thus, the buoyancy force term W is mainly driven by the term $-PS$, and then the numerical treatment becomes unstable. The case of $s_\infty = 25.4$ is the highest level at which
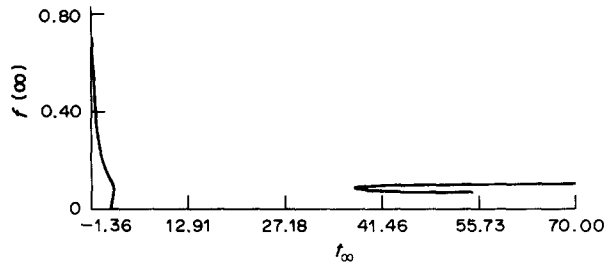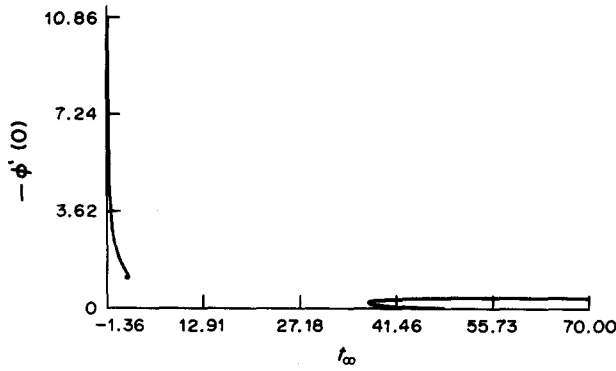

Fig. 4(a). Bifurcation diagram of parameter space of representation of solutions of the problems $P_{s_\infty}^+$ and $P_{s_\infty}^-$ in terms of $f(\infty)$ and t_∞ when $s_\infty = 25.4$.
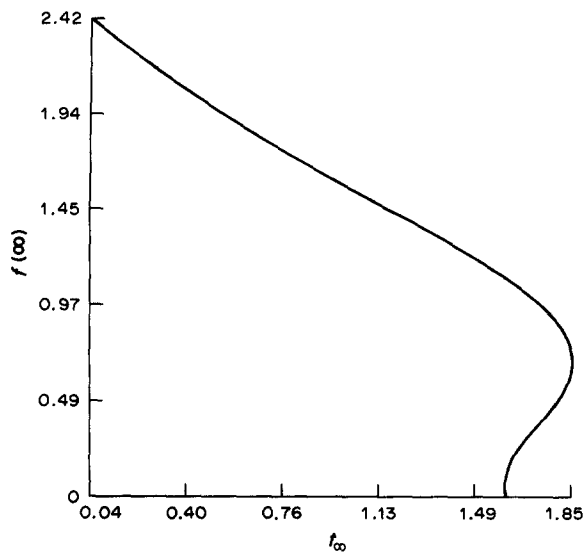
Fig. 4(a'). Details of parameter space representation of multiple solutions to the problem $P_{s_\infty}^+$ in terms of $f(\infty)$ and t_∞ when $s_\infty = 25.4$.

Fig. 4(b). Bifurcation diagram of parameter space of representation of solutions of the problems $P_{s_\infty}^+$ and $P_{s_\infty}^-$ in terms of $-\phi'(0)$ and t_∞ when $s_\infty = 25.4$.

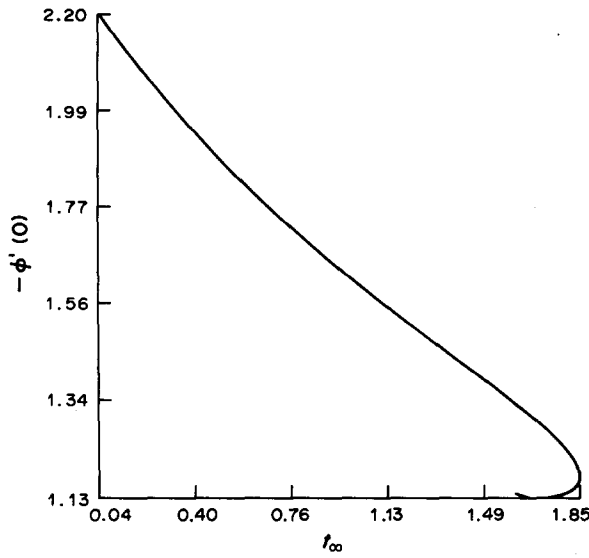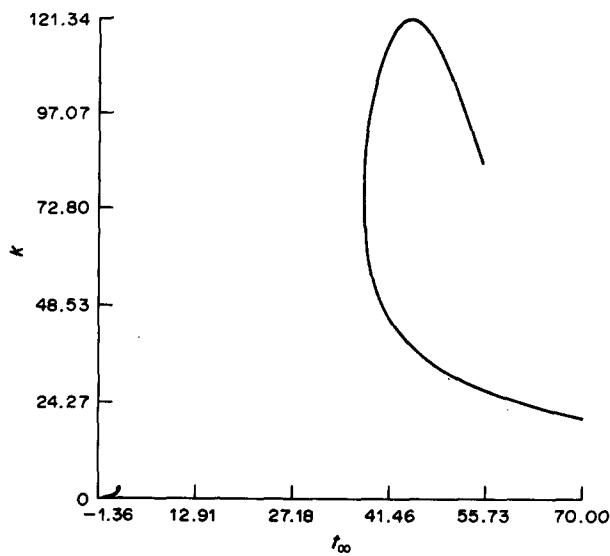Fig. 4(b'). Details of parameter space representation of multiple solutions to the problem $P_{s_\infty}^+$ in terms of $-\phi'(0)$ and t_∞ when $s_\infty = 25.4$.

Fig. 4(c). Bifurcation diagram of parameter space of representation of solutions of the problems $P_{s_\infty}^+$ and $P_{s_\infty}^-$ in terms of k and t_∞ when $s_\infty = 25.4$.
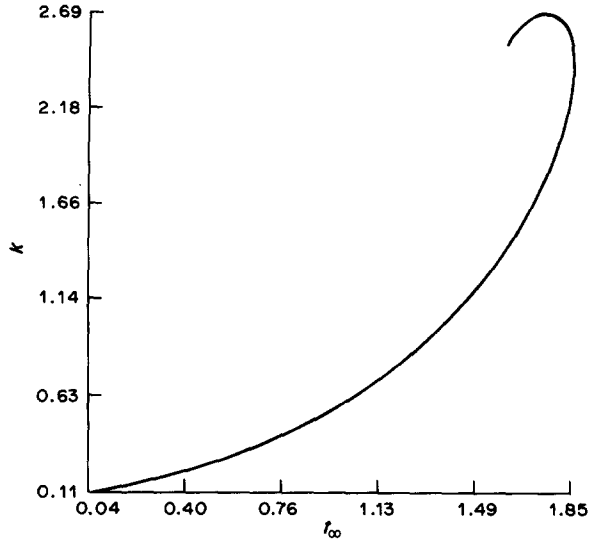
Fig. 4(c′). Details of parameter space representation of multiple solutions to the problem $P_{s_\infty}^+$ in terms of k and t_∞ when $s_\infty = 25.4$.
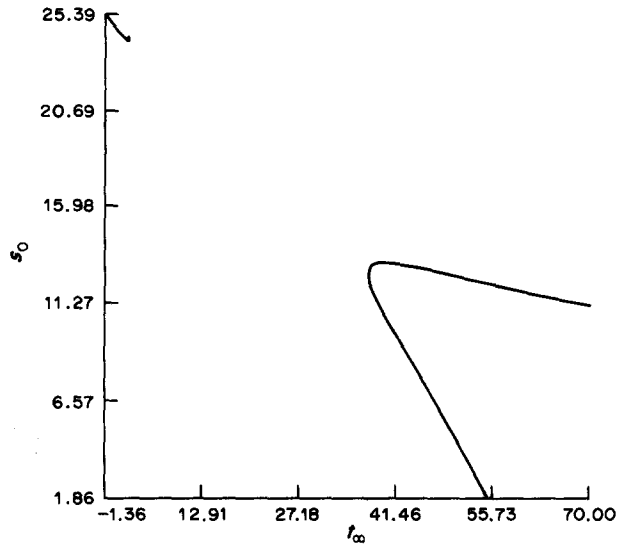

Fig. 4(d). Bifurcation diagram of parameter space of representation of solutions of the problems $P_{s_\infty}^+$ and $P_{s_\infty}^-$ in terms of s_0 and t_∞ when $s_\infty = 25.4$.
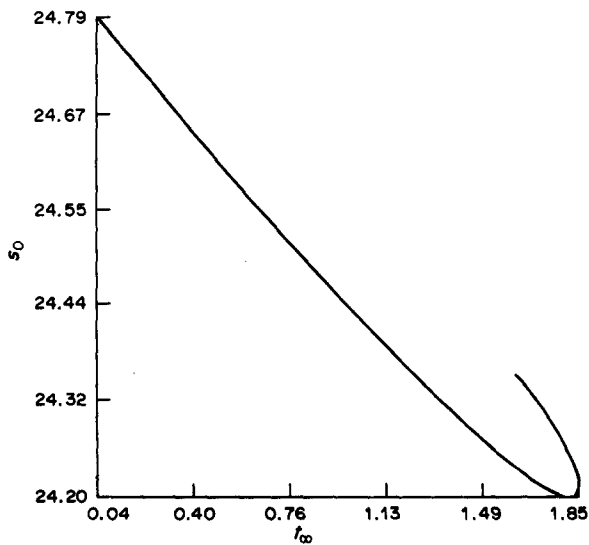

Fig. 4(d′). Details of parameter space representation of mulpitle solutions to the problem $P_{s_\infty}^+$ in terms of s_0 and t_∞ when $s_\infty = 25.4$.
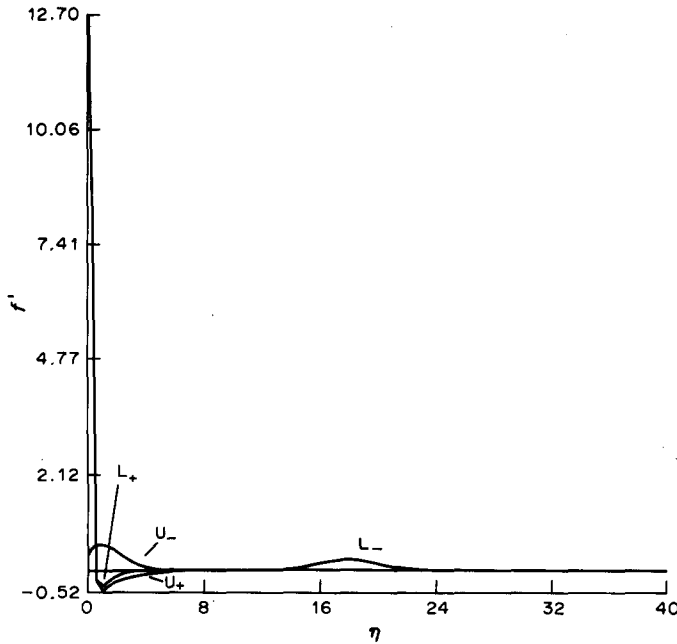
Fig. 5. Selected vertical velocity component distribution, f', for the problems $P_{s_\infty}^+$ and $p_{s_\infty}^-$ when $s_\infty = 25.4$. In the left region, at $t_\infty = 1.64034$, U_+ and L_+ are the upper and lower solutions, respectively, $\phi'_{U_+}(0) = -1.321084$ and $\phi'_{L_+}(0) = -1.131652$. In the right region, at $t_\infty = 55$, U_- and L_- are the upper and lower solutions, respectively, $\phi'_{U_-}(0) = -0.378090$ and $\phi'_{L_-}(0) = -0.001361$.

we have obtained both families of solutions for $P_{s_\infty}^+$ and $P_{s_\infty}^-$ successfully, and bifurcation diagrams are plotted in Figs 4(a–d'). Also, $-P$ ranges from 10 to 2.5×10^{-6} for $P_{s_\infty}^+$ at this salinity level. To the problem $P_{s_\infty}^+$, the numerical instability seems to be overcome by reformulating the similarity transformation as in Ref. [9], but it is reported that the occurrence of t_m exists only up to 26 p.p.t. for the problem $P_{s_\infty}^-$, it is believed that the solutions are obtainable if s_∞ is further increased up
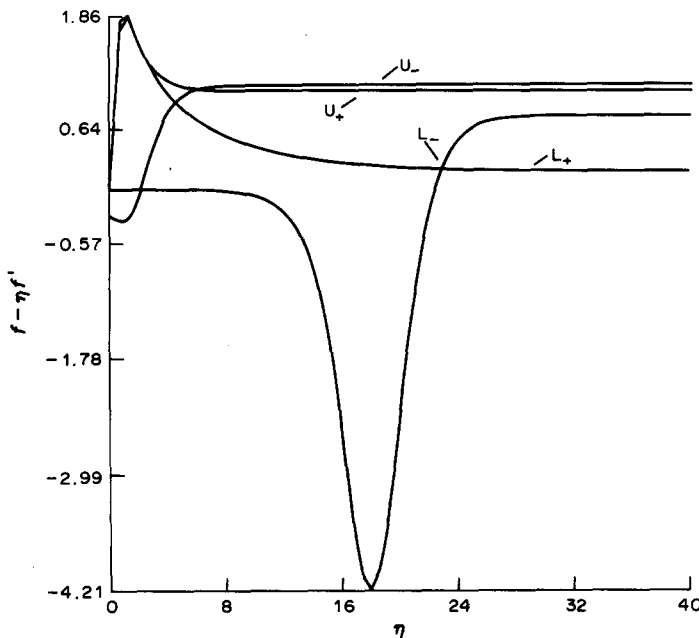

Fig. 6. Selected horizontal velocity component distributions, $f-\eta f'$, for the problems $P_{s_\infty}^+$ and $P_{s_\infty}^-$ when $s_\infty = 25.4$. In the left region, at $t_\infty = 1.64034$, U_+ and L_+ are the upper and lower solutions, respectively $\phi'_{U_+}(0) - 1.321084$ and $\phi'_{L_+}(0) = -1.131652$. In the right region, at $t_\infty = 55$, U_- and L_- are the upper and lower solutions, respectively, $\phi'_{U_-}(0) = -0.378090$ and $\phi'_{L_-}(0) = -0.001361$.

Fig. 7. Selected temperature distributions, ϕ, for the problems $P_{s_\infty}^+$ and $P_{s_\infty}^-$ when $s_\infty = 25.4$. In the left region, at $t_\infty = 1.64034$, U_+ and L_+ are the upper and lower solutions, respectively, $\phi'_{U_+}(0) = -1.321084$ and $\phi'_{L_+}(0) = -1.1311652$. In the right region, at $t_\infty = 55$, U_- and L_- are the uper and lower solutions, respectively, $\phi'_{U_-}(0) = -0.378090$ and $\phi'_{L_-}(0) = 0.001361$.
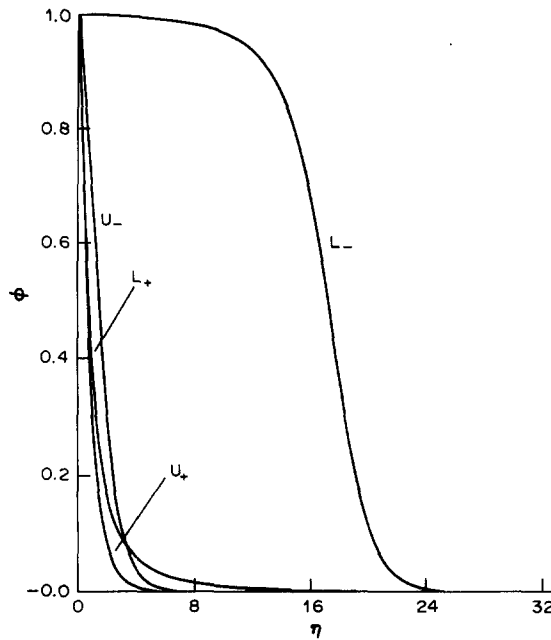
to at least the sea water level 35 p.p.t. and the upper edge $t_2(s_\infty)$ of the gap is much greater than 40°C. However, it is not practical in nature.

By treating P_{s_∞} as an initial value problem, METAN1 is used to integrate the equations (16–18) on $[0, \eta]$ with the initial conditions obtained from the data of Q_{s_∞}. Reasonable agreement is
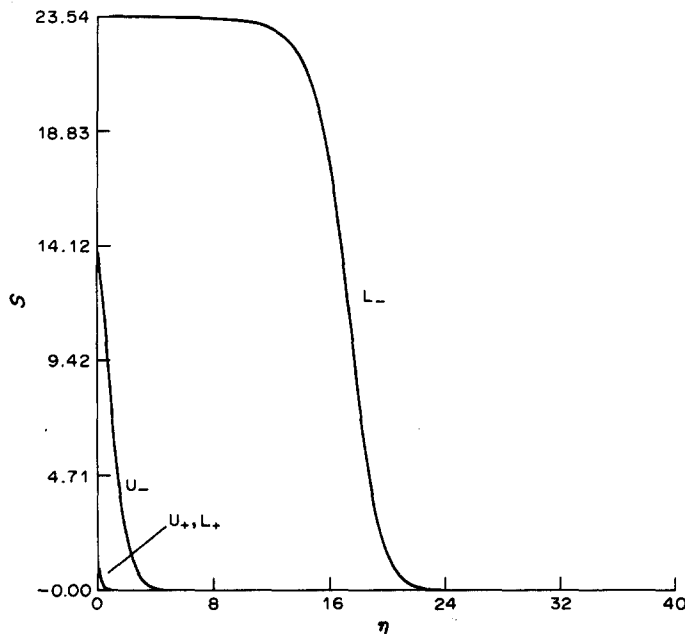

Fig. 8. Selected salinity distributions, S, $S(0) = (s_\infty - s_0)/s1$, for the problem $P_{s_\infty}^+$ and $P_{s_\infty}^-$ when $s_\infty = 25.4$. In the left region, at $t_\infty = 1.64034$, U_+ and L_+ are the upper and lower solutions, respectively, $\phi'_{U_+}(0) = -1.321084$ and $\phi'_{L_+}(0) = -1.131652$. In the right region, at $t_\infty = 55$, U_- and L_- are the upper and lower solutions, respectively, $\phi'_{U_-}(0) = -0.378090$ and $\phi'_{L_-}(0) = -0.001361$.

gradually reached by increasing η_∞ from 80, 100, 200, ..., 800. Selected graphs of velocity, temperature and salinity profiles are plotted in Figs 5–8 at $s_\infty = 25.4$.

4. CONCLUSIONS AND ADDITIONAL OBSERVATIONS

Numerical computations show that buoyancy force and flow reversals arise in a range $t_m(s_0) \leqslant t_\infty \leqslant \bar{t}_\infty(s_\infty)$, where $\bar{t}_\infty(0) = 2t_m(0)$. Although no experimental results have been reported on this subject, our result indicates that complicated mechanisms may arise and suggests that further experimental investigations are needed.

It is found that the width of gap in t_∞, $t_1(s_\infty) < t_\infty < t_2(s_\infty)$, increases in s_∞. The bounds of the gap are about 4.9811 and 6.7429; 3.8463 and 9.3450; 2.5564 and 33; 1.8514 adn 37.5 for $s_\infty = 0$, 10, 20 and 25.4, respectively. Moreover, the mathematical verification has shown the existence of the gap for s_∞ small. However, the boundary layer similarity transformations give no guidance in predicting buoyancy-driven transport for conditions that falls in this gap. A new formulation is necessary to describe such flows. Moreover, the phenomena to be described here are not known. Experimental study of such flows must guide the development of new mathematical model. Similar situation has occurs in the study presented by Gebhart et al. [4].

Multiple solution found here are remarkable in several respects. They appeared mainly outside the upper and lower bounds of gap. Pairs of multiple solutions in the left hand region, close to the lower edge of the gap, are very similar. These flows have a buoyancy reversal in the outer region of the layers. On the other hand, outside the upper edge of the gap, the upper and lower solutions are very different. The lower solution exhibits a thick layer near the interface surface. This insulates the surface, and results a huge decrease in heat transfer and interchange of mass of ice and salt at the interface. For example, $-\phi'_U(0)/-\phi'_L(0) \approx 36321$ at $t_\infty \approx 7.3841$ for the pure water case; $\phi'_U(0)/-\phi'_L(0) \approx 370$ at $t_\infty = 55$ for the case $s_\infty = 25.4$. Those quantities with subscripts U and L denote the upper and lower solution described above. It can be seen that the layer becomes thicker as t_∞ increases. This results the decrease of s_0 of the lower solution since the fluid inside the layer is less saline due to the insulation.

The multiple solutions have considerable different characteristics. This raises additional questions in interpreting such results in relation to any actual circulation in a porous medium. The steady flow might actually rise matters later in the left region although the existence of two solutions probably means instability. However, in the right region, the difference in the effects of steady transport would be great. For example, the large differences in the $\phi(\eta)$ and $s(\eta)$ distributions mean large differences in the buoyancy force associated with the different flows at the same t_∞. This means that a large amount of energy is potentially available for amplification for disturbance and vigorous effects may arise.

Unfortunately, as in Ref. [4], we know of no data from experimental measurements concerning transports in porous medium. Therefore, further understandings concerning flow instability and more inclusive may require an experimental data base.

REFERENCES

1. B. Gebhart and J. C. Mollendorf, Buoyancy-induced flows in water under conditions in which density extremum may arise. *J. Fluid Mech.* **89**, 673–707 (1978).
2. J. Ramilison and Gebhart, Buoyancy-induced transport in porous media saturated with pure or saline water at low temperature. *Int. J. Heat Mass Transfer* **23**, 1521–1530 (1980).
3. B. Gebhart and J. C. Mollendorf, A. new density for pure and saline water. *Deep Sea Res.* **24**, 831–841 (1977).
4. B. Gebhart, B. Hassard, S. Hastings and N. Kazarinoff, Multiple steady state solutions for buoyancy-induced transport in porous media saturated with cold pure and saline water. *Numer. Heat Transfer*, **6**, 337–352 (1983).
5. S. P. Hastings and N. D. Kazarinoff, Multiple solutions for a problem in buoyancy-induced flow. *Archs ration. Mech. Analysis* (in press).
6. V. P. Carey, Transport in vertical mixed convection flows and natural convection flows in cold water, Ph.D Thesis, SUNY at Buffalo, N.Y. (1981).
7. K. Fujino, E. L. Lewis and R. G. Perkin, The freezing point of sea water at pressure up to 1000 bars. *J. geophys. Res.* **79**, 1792–1797 (1974).
8. J. Bear, *Dynamics of Fluid in Porous Media*, pp. 647–651. Elsevier, New York (1972).
9. D. R. Caldwell, Thermal conductivity of sea water. *Deep–Sea Res.* **21**, 131–137 (1974).
10. H. W. Somerton, Some thermal characteristics of porous rocks. *J. Petrol. Technol.* **10** (Note 2008), 61–64 (1958).

11. L. A. Bromley, V. A. Desaussure, J. C. Clipp and J. S. Wright, Heat capacities of sea water solutions at salinities of 1 to 12% and temperatures of 2° to 80°C. *J. chem. Engng Data* **12** (2), 202–206 (1967).
12. P. Deuflhard, *Recent Advances in Multiple Shooting Techniques for Ordinary Differential Equations,* pp. 217–272. Academic, New York (1980).
13. R. Bulirsch, Die Mehrziemethode zur Numerischen Loesung von Niichtliearen Pandwertproblemen und Aufgaben der Optimalen Steuerung, Carl–Cranz–Gesellschaft: Technical Report (1971).
14. P. Deuflhard, A. modified Newton method for the solution of ill-conditioned systems of nonlinear equations with application to multiple shooting. *Numer. Math.* **22,** 289–315 (1974).
15. J. Stoer and R. Bulirsch, *Einfuehrung in die Numerisch Mathematik II,* 1st edn. Springer, Berlin (1973).
16. P. Deuflhard, Order and stepsize control in extrapolation methods. Technical Report Univ. Heidelberg, Vol. 93 5FB 123, (1980)
17. P. Deuflhard and G. Bader, Multiple shooting techniques revised. Technical Report Vol. 163, Univ. Heidelberg, SFB 123 (1982).
18. G. Bader and P. Deuflhard, A semi-implicit midpoint rule for stiff systems of ordinary differential equations. Technical Report Vol. 114, Heidelberg, SFB 123 (1981).
19. C. A. Wang, Multiple steady state solutions of buoyancy induced flows of a vertical ice wall melting in porous media saturated with pure and saline water. Ph.D Thesis, SUNY at Buffalo, N.Y. (1985).